18TH WORLD CONFERENCE ON EARTHQUAKE ENGINEERING
WCEE2024
MILAN

MILAN, ITALY
30TH JUNE - 5TH JULY 2024
www.wcee2024.it

SEISMIC RETROFITTING OF STEEL MRFs WITH EXTERNAL BRBs: PRELIMINARY EXPERIMENTAL & NUMERICAL RESULTS

F. Freddi[1], L. Di Sarno[2], M. D'Aniello[3], O-S. Kwon[4], R. Landolfo[3], S. Bousias[5], J-R. Wu[2], M. Cicia[3], F. Gutiérrez-Urzúa[1], J. Park[4], N. Stathas[5] & E. Strepelias[5]

[1] Dept. Civil, Env. & Geomatic Engineering, University College London, London, UK, f.freddi@ucl.ac.uk

[2] Dept. Civil and Environmental Engineering, University of Liverpool, Liverpool, UK

[3] Dept. Structures for Engineering & Architecture, University of Naples Federico II, Naples, Italy

[4] Dept. Civil & Mineral Engineering, University of Toronto, Toronto, Canada

[5] Structures Laboratory (STRULAB), Civil Engineering Dept., University of Patras, Patras, Greece

Abstract: *The use of buckling-restrained braces (BRBs) represents an effective retrofit strategy to significantly improve the seismic performance of existing structures. BRBs can be included within the existing frames, creating an additional load path and contributing to their strength, stiffness, and energy dissipation capacity. However, BRBs are typically placed inside the structural frame mesh, thus requiring the demolition and reconstruction of non-structural components to be installed. The present study explores the seismic retrofitting of existing steel structures, considering an external placement of the BRBs to minimise the intervention's invasiveness and, consequently, business interruptions and indirect losses. A two-storey steel moment-resisting frame (MRF) designed primarily for gravity loads and retrofitted with BRBs placed externally to the frames was considered as case study. The research includes large-scale Pseudo-Dynamic (PsD) tests performed as part of the HITFRAMES (i.e., HybrId Testing of an Existing Steel Frame with Infills under Multiple EarthquakeS) SERA project. The experimental results provided significant insights into the seismic response of the retrofitted structure and allowed the calibration of advanced 3D Finite Element (FE) models in ABAQUS. The results provide insights into the effective implementation of this retrofit solution and the influence of BRBs eccentricity to the seismic response.*

1. Introduction

Post-earthquake field investigations continuously highlighted the seismic vulnerability of existing structures designed prior to the introduction of modern seismic design codes (*e.g.,* Gómez *et al.,* 2015; Di Sarno *et al.,* 2018; Di Sarno and Wu 2020; Freddi *et al.,* 2021). Typical damage observed on exiting steel moment resisting frames (MRFs) includes the formation of plastic hinges in the columns, yielding of the panel zones at beam-column connections, and soft-storey mechanisms (*e.g.,* Gutiérrez-Urzúa *et al.,* 2021). It is nowadays essential to develop reliable retrofit strategies to effectively increase the seismic performance of such structures.

In this context, the use of buckling-restrained braces (BRBs) represents an effective strategy to increase the seismic performance of existing structures, including their lateral strength, stiffness, and energy dissipation capacity (*e.g.,* Soong and Spencer 2002). BRBs are passive energy dissipative devices typically incorporated within a bracing system (Xie 2005). Such devices contain a yielding core confined by a sleeve, providing

buckling resistance and allowing them to experience large inelastic deformations both in tension and compression, showing an almost symmetric behaviour (Zona and Dall'Asta 2012). Several experimental studies investigated the local response of BRBs (*e.g.,* Tremblay *et al.,* 2006) and their effectiveness in the seismic retrofit of reinforced-concrete (RC) (*e.g.,* Di Sarno and Manfredi 2012; Della Corte *et al.,* 2015; Wu *et al.,* 2017; Ozcelik and Erdil 2019) and steel frames (*e.g.,* Fahnestock *et al.,* 2003; Lin *et al.,* 2012; Khoo *et al.,* 2016; Mojiri *et al.,* 2021). Additionally, extensive numerical studies have also been conducted to assess the seismic performance of BRB-retrofitted framed structures (*e.g.,* Di Sarno and Elnashai 2009; Di Sarno and Manfredi 2010; Zona *et al.,* 2012; Güneyisi 2012; Freddi *et al.,* 2013 and 2021; Castaldo *et al.,* 2021) and explore their optimal design and placement (*e.g.,* Ragni *et al.,* 2011; Sutcu *et al.,* 2014; Barbagallo *et al.,* 2016; Freddi *et al.,* 2021; Gutiérrez-Urzúa and Freddi 2022).

BRBs are commonly installed aligned with the plane of the frames, requiring the removal of non-structural components, such as the infill walls, as part of the retrofit intervention. This operation typically implies lengthy business interruptions and represents one of the main limitations to the application of this retrofit strategy. Several innovative strategies, such as the use of exoskeletons or dissipative towers (*e.g.,* Di Lorenzo *et al.,* 2023; Gioiella *et al.,* 2018), have been recently investigated to overcome such limitations. In such solutions, the existing structure is retrofitted with braces placed externally to the frame or by connecting the structure to a parallel system, providing additional stiffness, strength, and ductility. Such solutions have the advantage of being implemented with minimal disturbance to the day-to-day use of the building. However, the use of exoskeletons equipped with dissipative devices, such as BRBs, has received limited attention.

In such solutions, the design of the connections is one of the most critical aspects, as it affects the ability of the BRBs to fully develop their ductility. Moreover, the failure modes of such connections may impair the global performance of the retrofitted structures. Guidance on the design of gusset plates for conventional BRBs connections can be found in the AISC standards (AISC 2016). However, there is still limited guidance on the design of these types of assemblies, and no prequalified connections have been developed for externally installed BRBs. Therefore, further investigation should be carried out in this regard.

This paper presents the preliminary work and results of a large-scale Pseudo-Dynamic (PsD) test performed on an existing steel MRF retrofitted with external BRBs. The tests were performed as part of the HITFRAMES (*i.e.,* HybrId Testing of an Existing Steel Frame with Infills under Multiple EarthquakeS) SERA project at the STRULAB of the University of Patras, Greece. The test specimen was a two-storey existing steel moment frame designed primarily for gravity loads and retrofitted with external BRBs. Significant attention was placed on the BRBs' connection details and their influence on the response of the tested frame. The experimental tests highlighted the significant torsional and distortional deformation in the parts of columns where the BRB connections were located, which was anticipated to be attributed to the BRBs eccentricity. Numerical simulations were performed by an advanced Finite Element (FE) model in ABAQUS (Dassault Systèmes 2014) to investigate the influence of the connection detail.

2. Case study structure

2.1. The prototype structure

The prototype structure consists of a two-storey, one-bay by three-bay non-seismically designed steel MRF. The building has a constant inter-storey height of 3.4 m and bay widths of 4.65 m and 8.65 m, respectively, along the *x*- and *y*-directions. The building was designed for gravity loads only following the European design code for steel buildings, Eurocode 3 (EC3), assuming a non-structural permanent load equal to 2.58 kN/m^2 and an imposed load equal to 3 kN/m^2. Wind load was considered negligible, leading to a complete lack of lateral loading resisting systems in the frame design. The steel profiles were HE 240 A, IPE 270, and IPE 200, respectively, for columns, primary and secondary beams, with the weak axis of columns in the *x*-direction. A steel grade S355 was adopted for beams and columns. All primary beams were connected to columns through full penetration welds, and columns were fixed at the base. A 200-mm-deep concrete slab was considered for each storey. The final mass of the prototype building was equal to 117.0 and 95.0 tons, respectively, for the first and second stories. The interested reader can refer to Di Sarno *et al.,* 2021 for additional details on the prototype structure.

2.2. The scaled structure

The prototype structure was scaled down by a factor $\lambda = 0.75$ for the experimental tests according to the lab capabilities. The model scaling was implemented assuming material scaling identity. As a result, the storey height and bay width of the steel frame were reduced to 2.5 and 3.5 m, respectively, and the profiles of columns and beams became HE180A and IPE200. The BRBs were installed in the central bay of the steel frame only; hence, a total of four BRBs were employed to retrofit the structure.

2.3. Codified assessment of the scaled structure

The seismic performance assessment of the scaled structure was conducted through non-linear static analyses according to the current Eurocode 8 - Part 3 (EC8-3). A two-dimensional FE model of the frame of the scaled structure in the *x*-direction was developed in OpenSees (McKenna *et al.,* 2011), accounting for both mechanical and geometric non-linearities. Beams and columns were modelled with a distributed plasticity approach using *'forceBeamColumn'* elements and fibre sections. The *'Steel01'* material was adopted for modelling beams and columns with a yield stress of 424 MPa and 2% hardening. Besides, fully rigid beam-column connections were assumed in the FE model, and the model was fixed at the base.

A modal analysis was performed to determine the natural periods and mode shapes of the frame. The results are presented in Table 1. Successively, pushover analyses were performed to assess the seismic performance of the building. The pushover analyses considered two lateral load patterns according to the EC8-3, namely 'uniform' and 'modal' patterns. The pushover curves of the prototype building are presented in Figure 1, including the roof drifts corresponding to the demands (indicated as unfilled dots) and capacities (filled dots) of each limit state defined in the EC8-3 (*i.e.,* Damage Limitation - DL, green dots, Significant Damage - SD, orange dots) and Near Collapse - NC, red dots). The seismic demands, *i.e.,* target displacements, were determined by following the N2 method employed in the Eurocode 8 (EC8-1), while the seismic capacities were determined by monitoring the end rotation of all beams and columns, according to the criteria in Table 2, which are defined in terms of multipliers of the yielding rotation θ_y of columns and beams. Both demands and capacities were represented by the roof drift herein. Figure 1 shows that the bare-scaled structure failed to fulfil the requirements for the DL and NC limit states; therefore, the retrofit was necessary to improve the seismic performance of the steel frame.

Table 1. Modal characteristics of the scaled structure.

Configuration	1st period [sec]	1st mode shape	Participating mass [%]
Bare	0.94	[0.428, 1.000]	85.27
Retrofitted	0.32	[0.545, 1.000]	91.64

Table 2. Capacity Limits for beams and columns according to EC8-3, valid only for v ≤ 0.3.

Cross section type	Limit States		
	Damage Limitation	Significant Damage	Near Collapse
Class 1	1.0 θ_y	6.0 θ_y	8.0 θ_y
Class 2	0.25 θ_y	2.0 θ_y	3.0 θ_y

2.4. Design of BRBs and numerical modelling

As per the EC8-3, the design of BRBs should allow the retrofitted steel MRF to meet the requirements of newly designed structures defined in the EC8-1. Two limit states are defined in EC8-1, namely the Ultimate Limit State (ULS) and the Damage Limit State (DLS), respectively, associated with return periods (T_R) equal to 475 years and 95 years. The ULS requires the design seismic forces in each structural component not to exceed the corresponding design resistance, whilst for cases with non-structural elements fixed in a way so as not to interfere with structural deformations, the DLS requires inter-storey drifts (d_r/h) not to exceed the value of 1%.

The properties of the BRB devices adopted in the present study are provided in Table 3, where K_e is the elastic stiffness, F_y is the force at first yielding, d_u is the maximum allowable axial displacement, $F_{1,T}$ and $F_{1,C}$ are the yielding forces at stable loops in tension and compression, and $F_{u,T}$ and $F_{u,C}$ are the maximum forces in tension and compression, respectively. The considered model of BRBs is shown in Figure 2. The BRB devices are arranged in series with an elastic brace to form the bracing system. A truss element was adopted to model the

axial behaviour of the BRB, while an elastic beam element was adopted to simulate the elastic brace. Besides, in order to overcome convergence issues, an additional elastic element with flexural and torsional capacity and negligible axial resistance was included in parallel to the BRB (Gutiérrez-Urzúa and Freddi 2022).

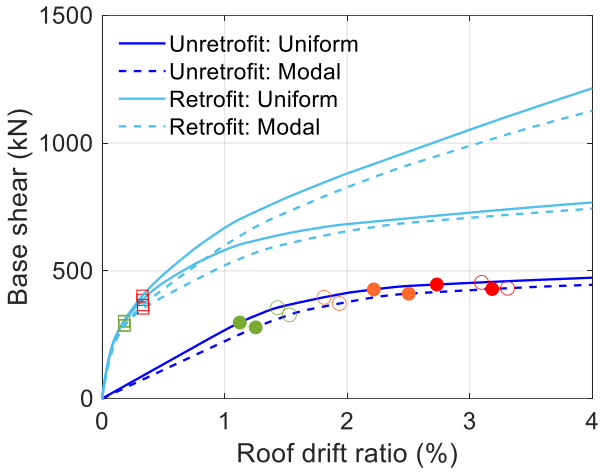

Figure 1. Pushover curves of the scaled structure with and without BRBs.

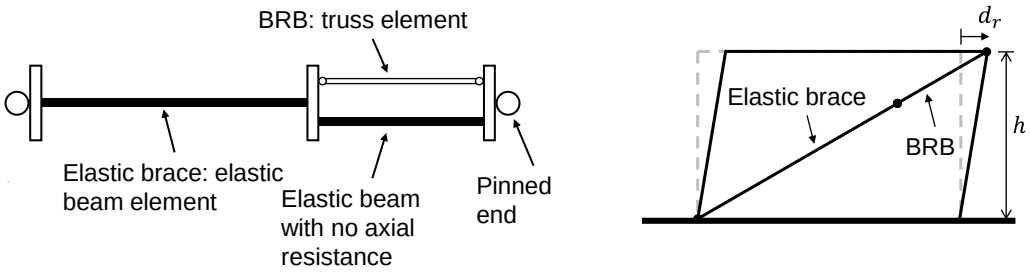

Figure 2. Model of the BRB brace in OpenSees.

Table 3. Property of the selected BRB for retrofitting the scaled structure.

K_e [kN/m]	F_y [kN]	d_u [mm]	Tension		Compression	
			$F_{1,T}$ [kN]	$F_{u,T}$ [kN]	$F_{1,C}$ [kN]	$F_{u,T}$ [kN]
88000	125	20	167	175	191	225

Figure 1 also shows the pushover curves of the retrofitted scaled structure. It is worth mentioning that two pushover analyses in opposite directions were performed for each lateral load pattern to account for the asymmetric behaviour of BRBs in tension and compression. Besides, as shown in Figure 1, the seismic demands were indicated by the unfilled 'squares' to highlight that they were determined based on the limit states in EC8-1 instead of EC8-3. Figure 1 shows that the use of BRBs significantly increased the lateral stiffness and strength of the scaled structure. The asymmetric behaviour of BRBs in tension and compression can also be anticipated from the pushover curves, where the retrofitted frame showed greater strength and hardening when the BRBs were activated in compression than in tension.

To check the performance of the BRBs-retrofitted frame with respect to the ULS, the bending moment demand-to-capacity ratios (DCRs) for all beams and columns were examined and shown in Figure 3. The demands were determined as the bending moment induced on each member at the target displacement for ULS. On the other hand, the determination of bending moment capacities took into account the interaction with axial and shear forces, according to the EC3-1. Figure 4 shows that all beams and columns satisfied the ULS requirements. The most critical bending moment demands were found to be concentrated on the columns on the lower floor, regardless of load pattern or direction, where the DCRs were approximately 0.4, while all other beams and columns showed a DCR lower than 0.2. In addition, the response of BRBs is presented in Figure

4. In all loading cases, the BRBs at the first storey experienced inelastic deformations at ULS, while the BRBs at the second storey remained almost elastic. Although this does not represent an optimal solution, this was due to the approach followed that aimed at keeping the BRBs at both stories the same. Moreover, the inter-storey drift ratio of the retrofitted scaled structure at the DLS is also represented in Table 4, which indicates that the inter-storey drift ratios at DLS were less than 1%.

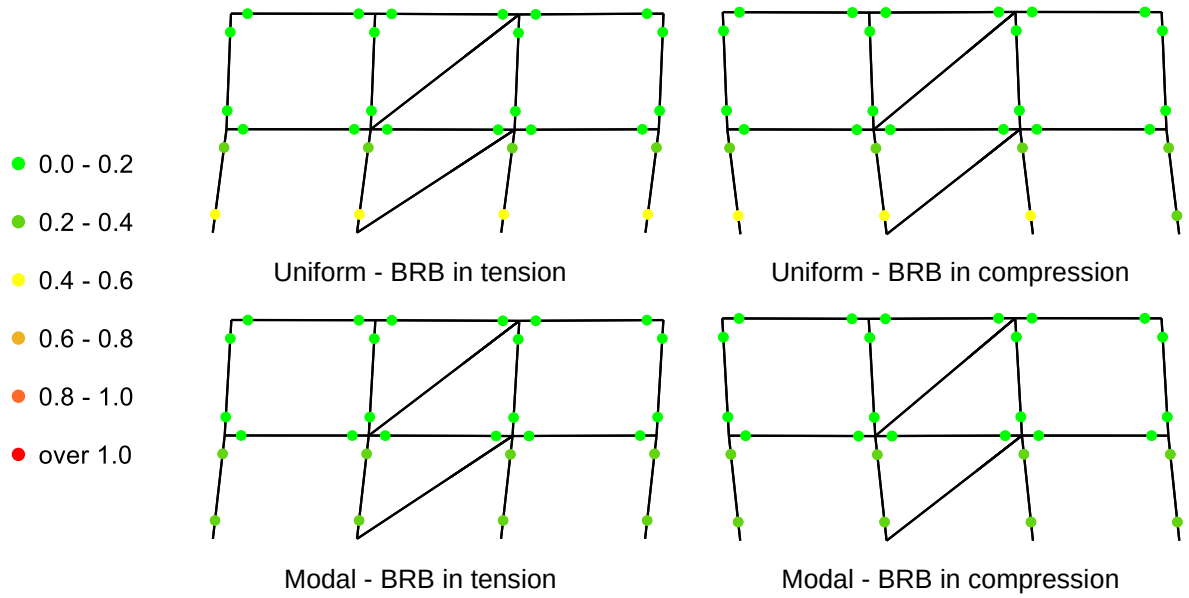

Figure 3. Damage state of the retrofitted scaled structure represented by the bending moment DCR for beams and columns.

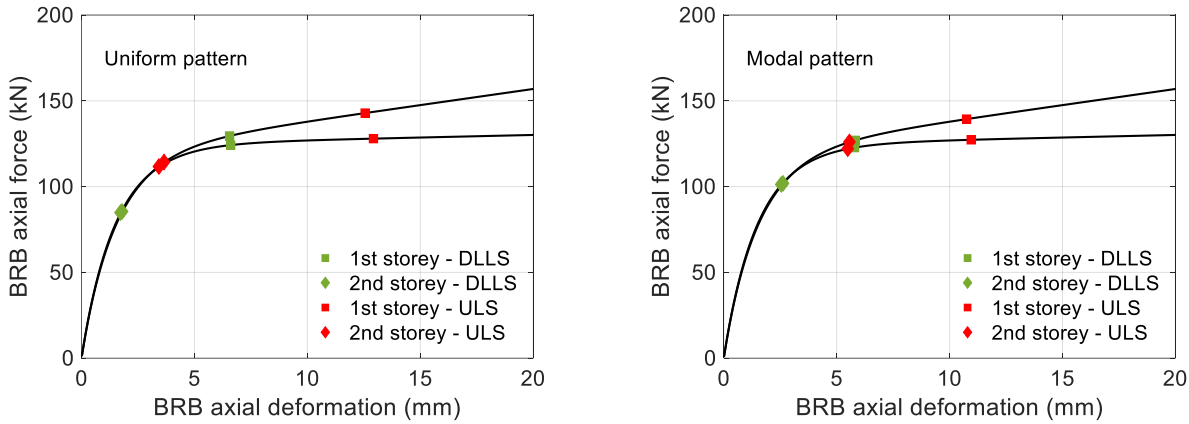

Figure 4. Monotonic behaviour of the BRBs under tension and compression and their deformation at DLS and ULS.

Table 4. Inter-storey drift ratio (d_r/h) of the retrofitted scaled structure at DLS.

	Uniform Pattern		Modal Pattern	
	Tension	**Compression**	**Tension**	**Compression**
1st storey	0.40 %	0.37 %	0.35 %	0.33 %
2nd storey	0.13 %	0.12 %	0.17 %	0.16 %

2.5. Design of BRBs connection

The above analyses were performed assuming the BRBs pinned to the beam-column intersection without accounting for the detailed modelling of the connection. In the test specimen, the BRB was connected to the column, as illustrated in Figure 5. The maxima effects due to the ultimate resistance of the BRBs (alternatively in tension and compression) were adopted to design the shear, bending, and torsional resistance of the bolted

end-plate connection. The eccentricity of the BRBs and its tilted position generate moments in both major and minor axes of the end-plate as well as shear force and torsion. The resistance of the end-plate was estimated in accordance with the component method as recommended by Eurocode 3 – Part 1.8 (EC3-1-8). However, the tension-shear interaction was considered for all bolts and their shear forces were evaluated assuming infinitive in-plane rigidity of the end-plate.

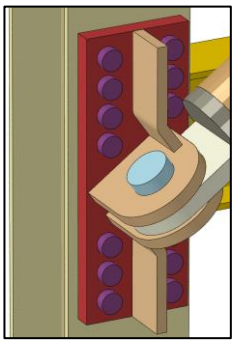

Figure 5: The design of the BRB-to-column connection.

3. Pseudo-Dynamic (PsD) Test

This chapter presents some details of the experimental campaign. The test specimen was a one-bay plane frame of the scaled structure. Two specimens were considered namely the bare and retrofitted test frame.

3.1. Test setup

Four actuators were used to conduct the PsD tests, with two connected to the slab at each storey. The connection between actuators and slabs was designed to ensure a smooth stress transfer from the actuators to the test frame. Two parallel tubular beams were placed on top of the column base plates and anchored to the strong floor of the lab to increase the rigidity of the base restraints of the test setup. The concrete slab was built following the erection of the steel frame. Figure 6 shows an overview of the specimen and several details of the bracing system, including the base plate connection, the connection of the BRB and the elastic brace, and the eccentric pin connections at the base and at the top. The specimen was extensively instrumented to monitor the response at the global and local levels. For the sake of brevity, only the storey displacements, the storey forces, and the response of the BRBs are provided hereinafter.

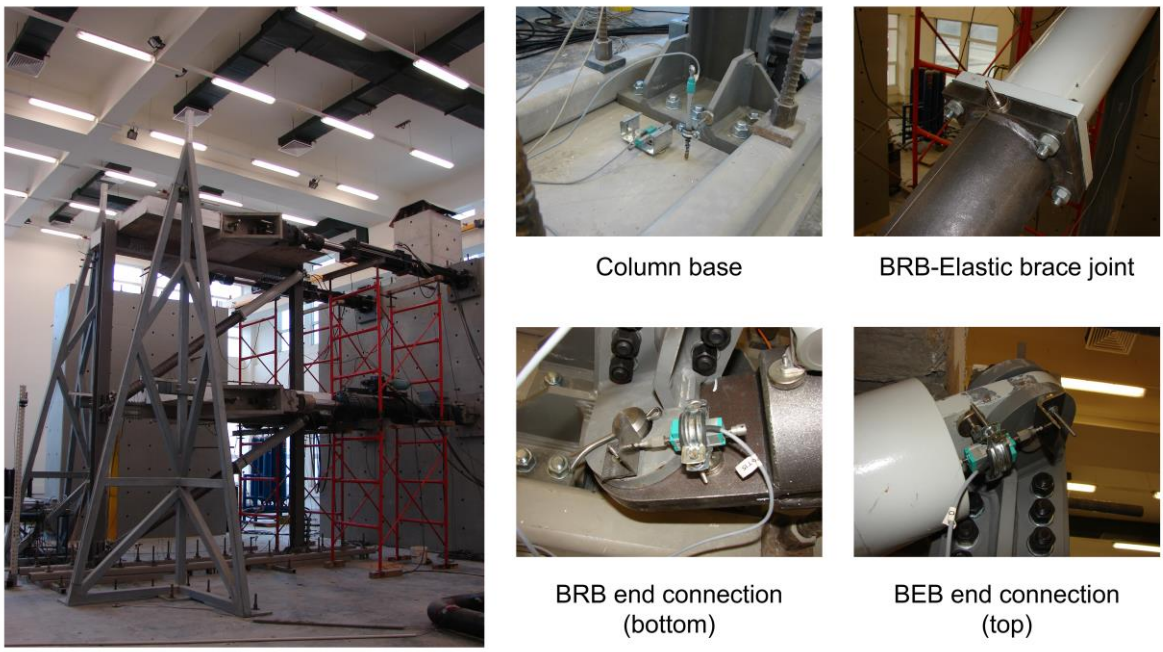

Figure 6. Test setup and details of the BRBs.

3.2. Ground motion selection

The PsD tests were performed considering the ground motion from the 24th of August 2016 at 1:36 am earthquake recorded at the Station of Norcia, Italy (NRC) in the East-West component (EMSC-20160824_0000006). The acceleration time histories were available from the Engineering Strong-Motion (EMS) database (Luzi *et al.,* 2015). This ground motion is considered representative of moderate-to-high seismicity of some areas in Southern Europe and was characterised by large spectral accelerations in the range of natural periods corresponding to the bare and retrofitted frames. The ground motion record was characterised by a moment magnitude (M_w) equal to 6.0, an epicentral distance (R_{epi}) equal to 15.3 km, and a peak ground acceleration (PGA) equal to 0.35g. It is noteworthy that the time of the GM record was scaled by a factor of 0.87 due to the model scaling.

3.3. Testing procedures

The PsD tests were conducted on the test frame via hybrid simulation (Kwon and Kammula, 2013). Hybrid testing allows the simulation of structures by representing critical components with physically tested specimens and the rest of the structure with numerical models. In this study, the investigated structure consisted of three bays along the *x*-direction. The hybrid tests numerically simulated the two external frames (not retrofitted with BRBs), while the central bay (with BRBs) was physically tested in the lab. In the numerical simulation, the two external frames were connected through a hinge to the central frame, neglecting the bending moments' contribution at beam-column connections.

The test matrix consisted of dynamic identification tests (*i.e.,* snap-back test) of the bare frame and a set of PsD tests with different ground motion intensities on the bare and retrofitted frames. Tests were conducted with incremental intensities of the selected ground motion record, with scaling factors (SF) ranging from 0.35 to 1.50. The present paper briefly discusses only the test of the retrofitted frame with SF = 1.0.

4. Tests' results and Finite Element (FE) simulations

Figure 7 shows the refined FE model of the test frame developed in ABAQUS. All steel components (*i.e.,* beams, columns, plates, and stiffeners) were modelled using the C3D8R solid element. The Young's modulus and Poisson's coefficient of steel were assumed to be 210 GPa and 0.3, respectively, while its plastic behaviour was defined by yield stress of 424 MPa and 2% hardening compatible with the simplified model in OpenSees. Beams were connected to the columns' web through tie constraints to simulate the full penetration welds. Moreover, the concrete slabs in the FE model were also modelled using the C3D8R solid element, which were simplified as homogeneous concrete blocks with an equivalent Young's modulus to simulate the rigidity of the RC slabs. The plastic behaviour of the concrete slabs was not defined in the present study since no obvious cracking was noticed during the tests. The slab was connected to the top flange of beams through tie constraints. Lastly, fixed boundary conditions were imposed on the bottom of columns and adjacent stiffeners. The BRBs and the elastic braces were modelled separately. The elastic braces were explicitly modelled as steel tubes, while the BRBs were simulated by two parallel axial connectors. The non-linear response of the simplified model for the BRBs was calibrated against experimental results.

Figure 8 shows the response of the test frame in terms of displacements and forces at the first and second floors. The numerical simulations were performed by applying to the FE models the same displacement histories recorded during the experimental tests (Figure 8a), which allows a direct comparison of the storey shear forces. It can be seen that the comparisons show a good agreement between the experimental tests and the FE simulations. Figure 9 presents the comparisons between the measured and estimated axial forces in BRBs, where the differences in the compressive forces were mainly attributed to the sliding of the pin connection of BRBs during the tests, which was not accounted for in the FE models.

The test results and numerical simulations highlighted the limitation of the current retrofit strategy and the need for careful consideration of the eccentric BRBs connection. Figure 10 shows the significant torsional and distortional deformation induced in the columns where BRB connections were located. To investigate the influence of the column deformability on the frame performance, four additional FE models were considered: *i)* bare frame model (BARE); *ii)* frame model with external BRBs (BRB_EXT); *iii)* frame model with in-plane BRBs (BRB_INP); *iv)* frame model with external BRBs and additional torsional and distortional constraints implemented on the column in the connection area (BRB_EXT_TCDC). Pushover analyses were conducted on these FE models and compared. Figure 11 shows the influence of the eccentric connection and the induced

torsional and distorsional effects on the lateral stiffness of the frame. The numerical results show that the external BRBs (BRB_EXT) contribute to increasing the stiffness and strength compared to the bare frame (BARE). However, the comparison with the frames with in-plane BRBs (BRB_INP) and with the additional constraints (BRB_EXT_TCDC) shows the significant stiffness reduction caused by the torsional and distortional effects of the columns. These preliminary results emphasise the importance of taking into account the deformability of the columns or to consider additional measures to increase the column's torsional stiffness and prevent the distortional deformation of the column flanges within the connection zones.

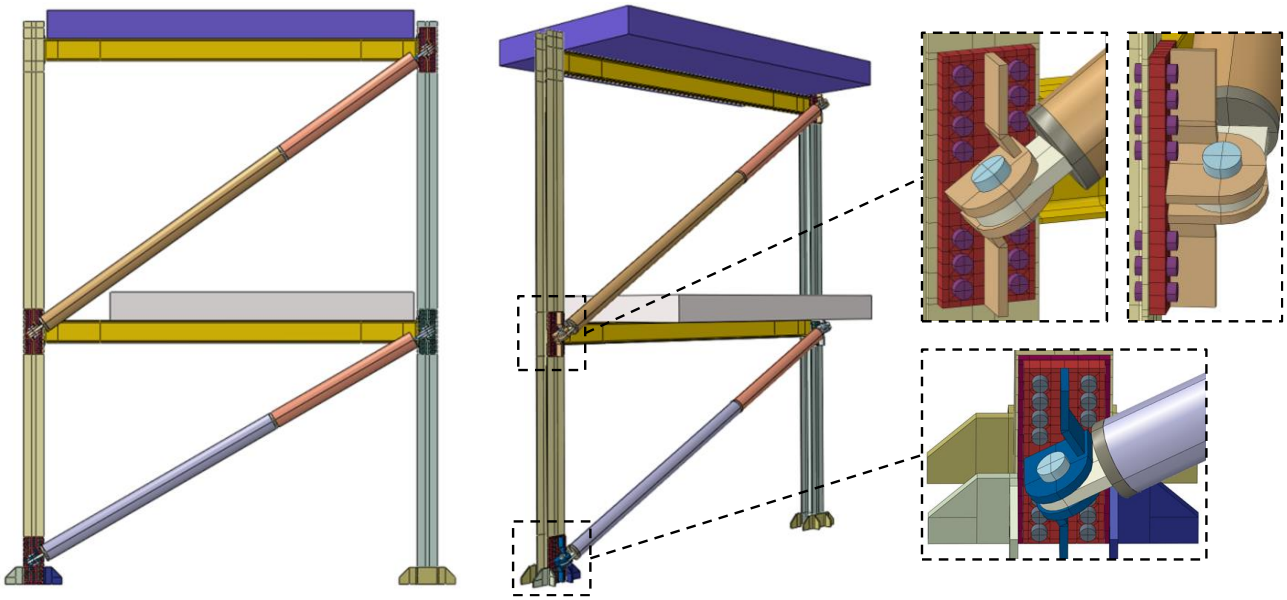

Figure 7. Finite Element (FE) modelling of the steel frame specimen retrofitted in ABAQUS.

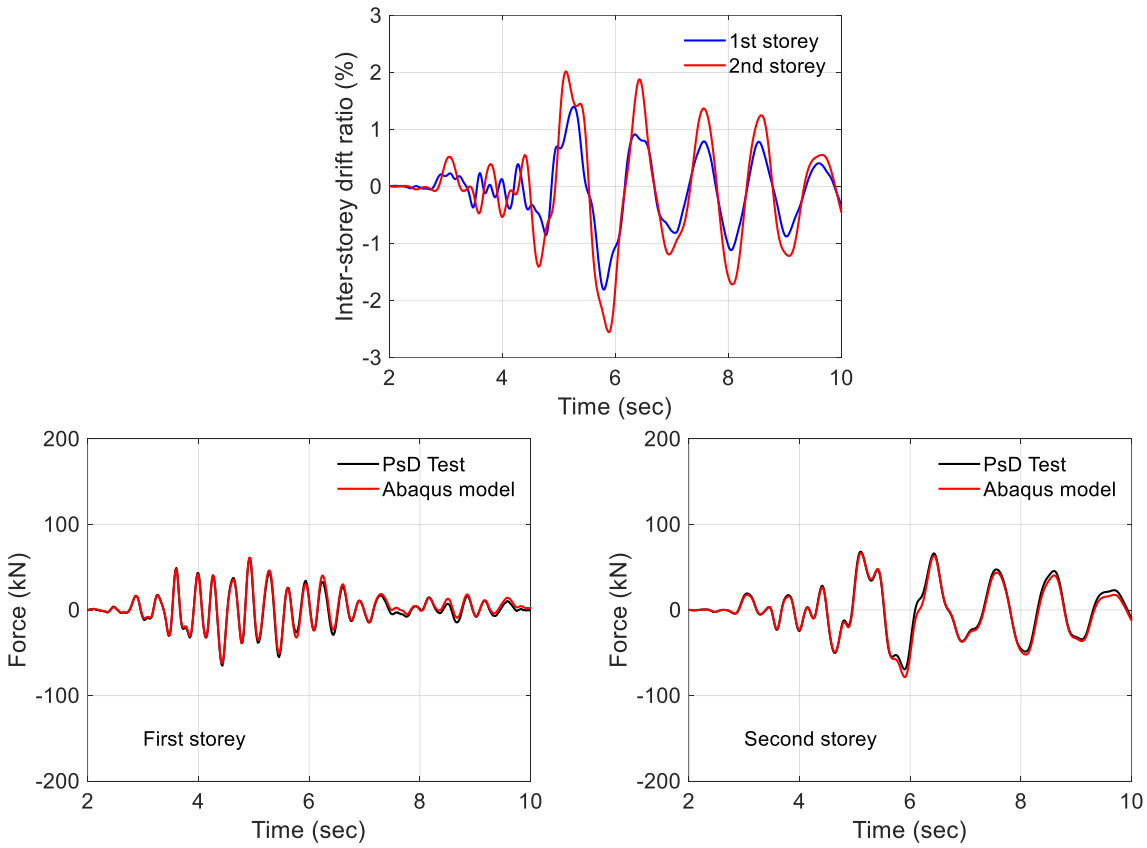

Figure 8. Displacement and forces of each storey of the retrofitted test frame.

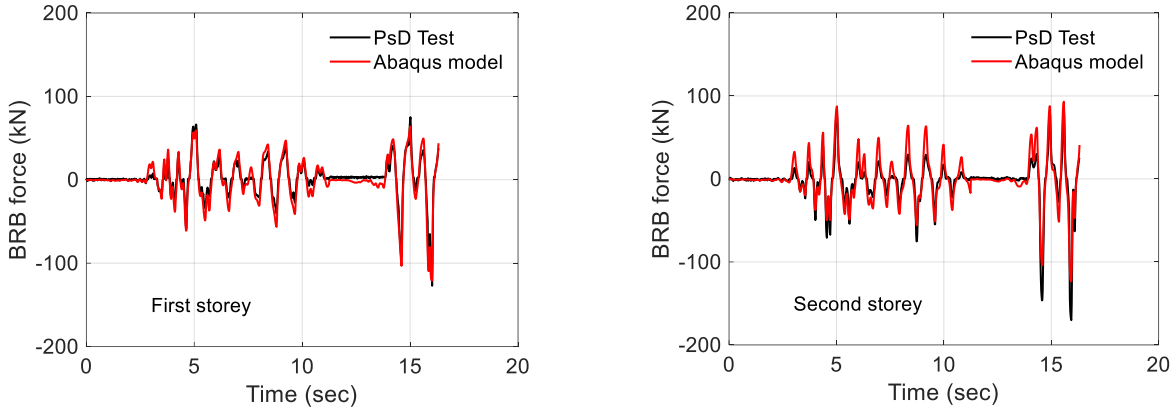

Figure 9. Comparison between the measured and estimated axial forces in BRBs.

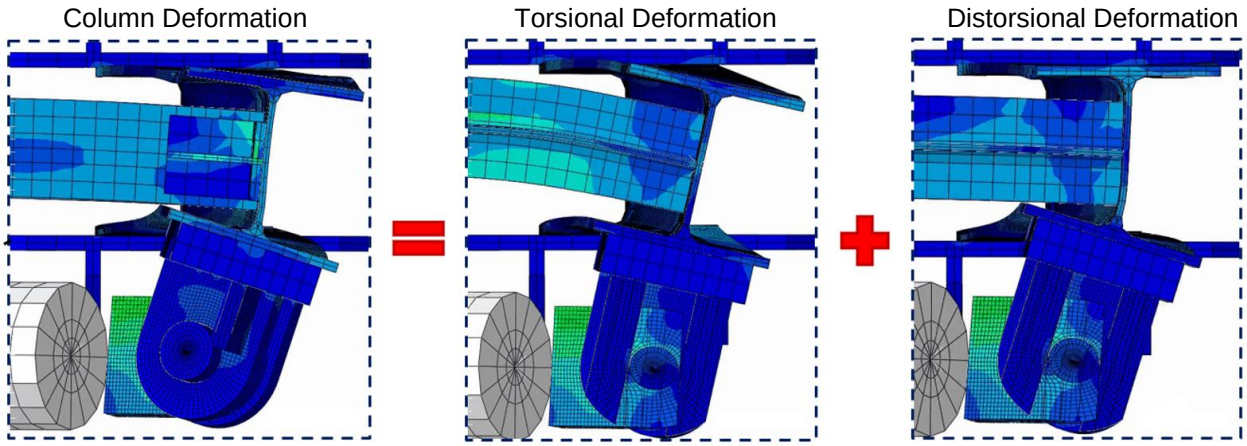

Figure 10. Torsional and Distortional Deformations of the column.

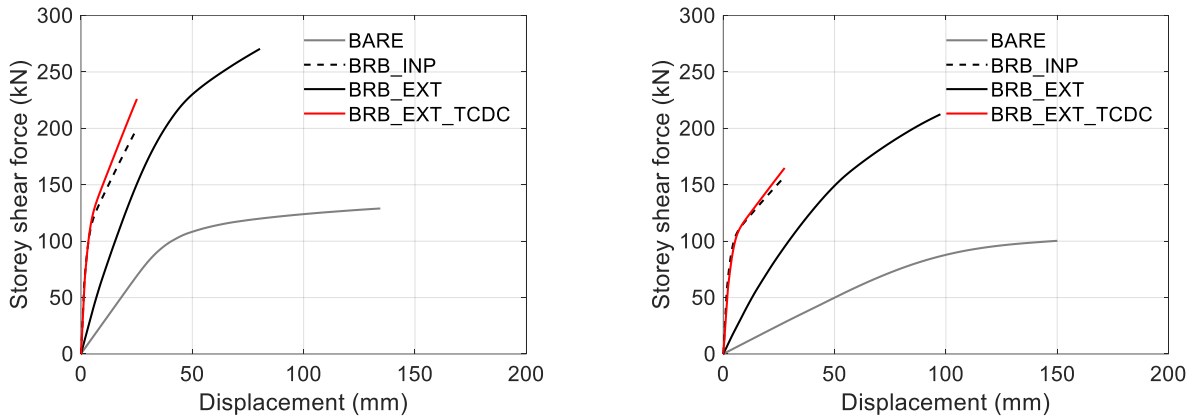

Figure 11. Comparison of the pushover curves of Model BRB_EXT_TCDC with the reference models: (a) first storey; (b) second storey.

5. Conclusions

This paper presents the design and results of a large-scale Pseudo-Dynamic (PsD) test performed on an existing steel MRF retrofitted with external BRBs. The tests were performed as part of the HITFRAMES (*i.e.,* HybrId Testing of an Existing Steel Frame with Infills under Multiple EarthquakeS) SERA project at the STRULAB of the University of Patras, Greece. The test specimen was a two-storey existing steel moment frame designed primarily for gravity loads and retrofitted with external BRBs. Numerical simulations were performed by an advanced Finite Element (FE) model in ABAQUS to investigate the influence of the connection detail. The experimental tests highlighted the significant deformations in the parts of columns where the BRB connections were located, which was anticipated to be attributed to the BRB eccentricity. It was found

that the eccentricity caused by the externally installed BRBs could lead to excessive torsional deformation of columns and distortional deformation of the flange where the BRB connections were located. Besides, the implementation of external BRBs without additional retrofit of the connections did not lead to the same performances resulting from the conventional retrofit solutions using in-plane BRBs, mainly due to the fact that external BRBs were not adequately activated at lower displacements as in the case of in-plane BRBs. Nonetheless, it was found that the performance of external BRBs could be approximately equivalent to the in-plane BRBs, providing that sufficient constraints were applied to restrain the torsional and distortional deformation of columns.

6. Acknowledgements

The financial support of the Seismic Engineering Research Infrastructure (SERA) project (European Commission, H2020-INFRAIA-2016-2017, Agreement No.730900) to HITFRAMES project is greatly acknowledged. Any opinions, findings and conclusions, or recommendations expressed in this paper are those of the Authors and do not necessarily reflect those of the sponsors.

7. References

AISC (2016). *ANSI/AISC 341-16: Seismic Provisions for Structural Steel Buildings*, American Institute of Steel Construction, Chicago, USA.

Barbagallo F., Bosco M., Marino E.M., Rossi P.P., Stramondo P.R. (2016). A multi-performance design method for seismic upgrading of existing RC frames by BRBs. *Earthquake Engineering and Structural Dynamics*, 46(7): 1099–1119.

Castaldo P., Tubaldi E., Selvi F., Gioiella L. (2021). Seismic performance of an existing RC structure retrofitted with buckling restrained braces. *Journal of Building Engineering*, 33:101688.

CEN (2005). *EN 1993-1-1:2005. Eurocode 3: Design of steel structures - Part 1-1: General rules and rules for buildings*, Comité Européen de Normalisation, Brussels.

CEN (2005). *EN 1993-1-8:2005. Eurocode 3: Design of steel structures - Part 1-8: Design of joints*, Comité Européen de Normalisation, Brussels.

CEN (2004). *EN 1998-1:2004. Eurocode 8: Design of structures for earthquake resistance - Part 1: General rules, seismic actions and rules for buildings*, Comité Européen de Normalisation, Brussels.

CEN (2005). *EN 1998-3:2005. Eurocode 8: Design of structures for earthquake resistance - Part 3: Assessment and retrofitting of buildings*, Comité Européen de Normalisation, Brussels.

Dassault Systèmes (2014). *ABAQUS/Standard User's Guide*, Version 6.14, Providence, USA.

Della Corte G., D'Aniello M., Landolfo R. (2015). Field testing of all-steel buckling-restrained braces applied to a damaged reinforced concrete building. *Journal of Structural Engineering*, 141(1): D4014004.

Di Lorenzo G., Tartaglia R., Prota A., Landolfo R. (2023). Design procedure for orthogonal steel exoskeleton structures for seismic strengthening. *Engineering Structures,* 275: 115252.

Di Sarno L., Elnashai A. (2009). Bracing systems for seismic retrofitting of steel frames. *Journal of Constructional Steel Research*, 65(2): 452–465.

Di Sarno L., Manfredi G. (2010). Seismic retrofitting with buckling restrained braces: Application to an existing non-ductile RC framed building. *Soil Dynamics and Earthquake Engineering*, 30(11): 1279–1297.

Di Sarno L., Manfredi G. (2012). Experimental Tests on Full-scale RC Unretrofitted Frame and Retrofitted with Buckling-restrained Braces. *Earthquake Engineering and Structural Dynamics*, 41(2): 315–333.

Di Sarno L., Paolacci F., Sextos AG. (2018). Seismic Performance Assessment of Existing Steel Buildings: A Case Study. *Key Engineering Materials*, 763: 1067-1076.

Di Sarno L., Wu J-R. (2020). Seismic assessment of existing steel frames with masonry infills. *Journal of Constructional Steel Research*, 169: 106040.

Di Sarno L., Freddi F., D'Aniello M., Kwon O.-S., Wu J.-R., Gutiérrez-Urzúa F., Landolfo R., Park J., Palios X., Strepelias E. (2021). Assessment of existing steel frames: Numerical study, pseudo-dynamic testing and influence of masonry infills. *Journal of Constructional Steel Research*, 185: 106873.

Fahnestock L.A., Sause R., Ricles J.M., Lu L.-W. (2003). Ductility demands on buckling-restrained braced frames under earthquake loading. *Earthquake Engineering and Engineering Vibration*, 2(2): 255-268.

Freddi F., Tubaldi E., Ragni L., Dall'Asta A. (2013). Probabilistic performance assessment of low-ductility reinforced concrete frames retrofitted with dissipative braces. *Earthquake Engineering and Structural Dynamics*, 42(7): 993–1011.

Freddi F., Ghosh J., Kotoky N., Raghunandan M. (2021). Device uncertainty propagation in low-ductility RC frames retrofitted with BRBs for seismic risk mitigation. *Earthquake Engineering and Structural Dynamics*, 50(9):2488-509.

Freddi F., Tubaldi E., Zona A., Dall'Asta A. (2021). Seismic performance of dual systems coupling moment-resisting and buckling-restrained braced frames. *Earthquake Engineering and Structural Dynamics*, 50(2): 329–353.

Freddi F., Novelli V., Gentile R., Veliu E., Andonov A., Andreev S., Greco F., Zhuleku E. (2021). Observations from the 26th November 2019 Albania Earthquake: the Earthquake Engineering Field Investigation Team (EEFIT) mission. *Bulletin of Earthquake Engineering*, 19(5): 2013–2044.

Gioiella L., Tubaldi E., Gara F., Dezi L., Dall'Asta. (2018). Modal properties and seismic behaviour of buildings equipped with external dissipative pinned rocking braced frames. *Engineering Structures*, 172: 807–8191.

Gómez L.V.D., Kwon O.-S., Dabirvaziri M.R. (2015). Seismic fragility of steel moment-resisting frames in Vancouver and Montreal designed in the 1960s, 1980s, and 2010. Canadian Journal of Civil Engineering, 42(11): 919-9294.

Güneyisi E.M. (2012). Seismic reliability of steel moment resisting framed buildings retrofitted with buckling restrained braces. *Earthquake Engineering and Structural Dynamics*, 41(5): 853–874.

Gutiérrez-Urzúa L.F., Freddi F., Di Sarno L. (2021). Comparative Analysis of Code Based Approaches for the Seismic Assessment of Existing Steel Moment Resisting Frames. *Journal of Constructional Steel Research*, 181: 106589.

Gutiérrez-Urzúa L.F., Freddi F. (2022). Influence of the design objectives on the seismic performance of steel moment resisting frames retrofitted with buckling restrained braces. *Earthquake Engineering and Structural Dynamics*, 51(13): 3131–3153.

Khoo H.H., Tsai K.C., Tsai C.Y., Tsai C.Y., Wang K.J. (2016). Bidirectional substructure pseudo-dynamic tests and analysis of a full-scale two-story buckling-restrained braced frame. *Earthquake Engineering and Structural Dynamics*, 45(7): 1085-107.

Kwon O.-S., Kammula V. (2013). Model updating method for substructure pseudo-dynamic hybrid simulation. *Earthquake Engineering and Structural Dynamics*, 42(13): 1971-1984.

Lin P.C., Tsai K.C., Wang K.J., Yu Y.J., Wei C.Y., Wu A.C., Tsai C.Y., Lin C.H., Chen J.C., Schellenberg A.H., Mahin S.A. (2012). Seismic design and hybrid tests of a full-scale three-story buckling-restrained braced frame using welded end connections and thin profile. *Earthquake Engineering and Structural Dynamics*, 41(5): 1001-20.

Luzi L., Puglia R., Russo E. (2015). ORFEUS Working Group 5. Engineering Strong Motion Database, Version 1.0, *Istituto Nazionale di Geofisica e Vulcanologia* (INGV). https://doi.org/10.13127/ESM

McKenna F., Scott M.H., Fenves G.L. (2010). Non-linear finite-element analysis software architecture using object composition, *Journal of Computing in Civil Engineering*, 24: 95-107.

Ozcelik R., Erdil EF. (2019). Pseudodynamic Test of a Deficient RC Frame Strengthened with Buckling Restrained Braces. *Earthquake Spectra*, 35(3): 1163–118.

Ragni L., Zona A., Dall'Asta A. (2011). Analytical expressions for preliminary design of dissipative bracing systems in steel frames. *Journal of Construction Steel Research*, 67(1): 102-113.

Mojiri S., Mortazavi P., Kwon O.-S., Christopoulos C. (2021). Seismic response evaluation of a five-story buckling-restrained braced frame using multi-element pseudo-dynamic hybrid simulations. *Earthquake Engineering and Structural Dynamics*, 50(12): 3243-326510.

Soong TT, Spencer BF. (2002). Supplemental energy dissipation: state-of-the-art and state-of-the-practice. *Engineering Structures*, 24(3): 243–259.

Sutcu F., Takeuchi T., Matsui R. (2014). Seismic retrofit design method for RC buildings using buckling-restrained braces and steel frames. *Journal of Constructional Steel Research*, 101: 304–313.

Tremblay R., Bolduc P., Neville R., DeVall R. (2006). Seismic testing and performance of buckling-restrained bracing systems. *Canadian Journal of Civil Engineering*, 33(2): 183–198.

Wu A.-C., Tsai K.-C., Yang H.-H., Huang J.-L., Li C.-H., Wang K.-J., Khoo H.-H. (2017). Hybrid experimental performance of a full-scale two-story buckling-restrained braced RC frame. *Earthquake Engineering and Structural Dynamics*, 46(8): 1223–1244.

Xie Q. (2005). State of the art of buckling-restrained braces in Asia. *Journal of Constructional Steel Research*, 61(6): 727–48.

Zona A., Dall'Asta A. (2012). Elastoplastic model for steel buckling-restrained braces. *Journal of Constructional Steel Research*, 68(1): 118–125.

Zona A., Ragni L., Dall'Asta A. (2012). Sensitivity-based study of the influence of brace over-strength distributions on the seismic response of steel frames with BRBs. *Engineering Structures*, 37(1): 179–192.